# VALIDATION OF THE CRAB-CAVITIES INTERNAL MONITORING STRATEGY

V. Rude, M. Duquenne, ESGT-CNAM, Le Mans, France
T. Dijoud, A. Herty, H. Mainaud Durand, M. Sosin, CERN, Geneva, Switzerland

*Abstract*

The high luminosity upgrade for the LHC at CERN (HL -LHC project [1], [2]) will extend the discovery potential of the LHC by a factor 10 [3]. It relies on key innovative technologies among which superconducting cavities for beam rotation, named "crab-cavities".

Alignment purposes of such RF cavities will involve a positioning to 0.5 mm at 3σ under harsh conditions. Two alignment monitoring systems have been compared and referenced to a laser tracker measurement in order to validate their accuracy under standard conditions (room temperature, atmospheric pressure, no radiation). In parallel, both systems are being validated regarding cryogenic and/or radiation aspect. This document presents the main results of the test campaign conducted in laboratory in order to validate the alignment strategy.

## INTRODUCTION

HL-LHC project aims at increasing the luminosity to the level of 250 $fb^{-1}$ per year (from 2024) with the goal of 3000 $fb^{-1}$. The process especially requires the use of transverse deflecting cavities, allowing the compensation of the crossing angle at the interaction points (IP) and increasing the luminosity [4]. HL-LHC upgrade assumes the installation of cryostats housing the superconducting crab-cavities (cf. Figure 1), distributed on both sides of ATLAS and CMS experiments (4 per IP).

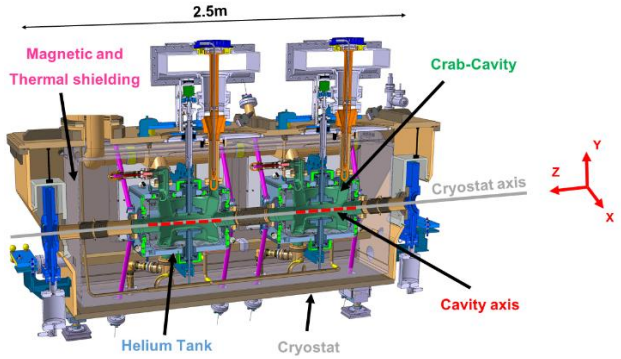


Figure 1 : Crab-cavities cryomodule (cross section)

Successful operation of the cavities will depend on their correct position and orientation defined from the following alignment constraints, given at 3σ:

- The cavities roll (Rz) w.r.t. the cryostat axis has to be lower than 5 mrad.
- The cavities pitch and yaw (Rx, Ry) w.r.t. the cryostat axis has to be lower than 1 mrad.
- The cavities axis has to be included in 0.5 mm diameter cylinder w.r.t. the cryostat axis.

In order to fulfil the alignment requirements, the accuracy of the position monitoring system has to be appropriately higher and it was chosen to be better than 50 µm [5]. Furthermore, the chosen system shall be compatible with the operating conditions of the cavities, including radiation dose in the range of 1 MGy/year, vacuum level of $10^{-6}$ mbar and cryogenics conditions at approximately 4 K.

Two independent monitoring systems were proposed as a baseline solution. One is based on Frequency Scanning Interferometry (FSI), able to perform measurements in the specific environment mentioned above. The second system relies on image acquisitions of reflective targets using a specific camera, called BCAM. This device will only be used for cross-checking measurements during the cooling down process, since the present radiation hardness of this technology is not high enough to fulfil the requirements.

This document aims at presenting the general approach to implement both monitoring systems for the cavities alignment purposes, as well as the comparison of their metrological performances (room temperature, atmospheric pressure, no radiation).

## DESCRIPTION OF MONITORING SYSTEMS

### *FSI system*

The FSI system is an absolute measuring interferometer developed for high precision and simultaneous absolute distance measurements [6]. In the zones that are concerned by radiations, the only components to be installed are components such as optical fibres, collimators, and reflective targets.

In simple terms, with the FSI technique, a distance measurement is deduced from the ratio between the phase change induced in an interferometer reference and an interferometer measurement by frequency scanning.

Based on the Absolute Multiline Technology (Etalon™ , Figure 2) [7], that should provide 0.5 ppm precision between 0.2 m and 20 m, the alignment monitoring of the crab-cavities will consist in determining the main axis of both cavities from a set of distance measurements along multiple lines of sight.

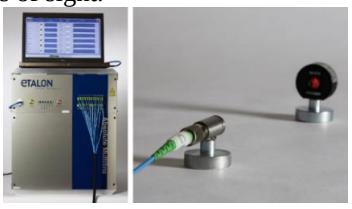


Figure 2 : Absolute Multiline Technology

The method will involve the distribution of reflective targets on the cavities flanges as well as the installation of specific optical feedthroughs holding the FSI collimators on the cryostat of the cryomodule, as presented in Figure 3.

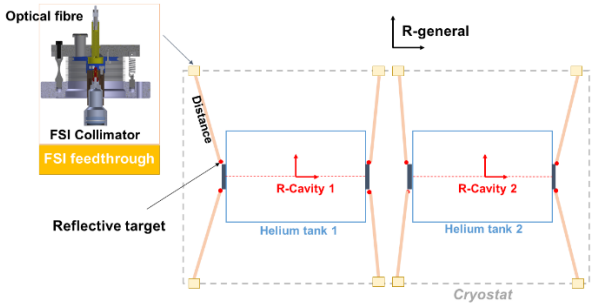


Figure 3 : FSI alignment system: schematic (longitudinal cross-section)

## *BCAM system*

The second monitoring system is based on image acquisitions of distributed light sources, using an optoelectronic device developed by Brandeis University [10]. In its simplest form, a BCAM (Brandeis Camera Angle Monitor) includes two light sources and a camera consisting of a lens and a CCD image sensor (cf. Figure 4).

An image acquisition provides the X and Y coordinates of a spot image projected onto the CCD, initially expressed in the CCD coordinate system. The vector connecting the spot image and the camera lens (i.e. pivot point) defines the bearing of the light source that can be expressed in different coordinate systems. The precision and accuracy of a BCAM indicated by the manufacturer are respectively 5 µrad and 50 µrad.

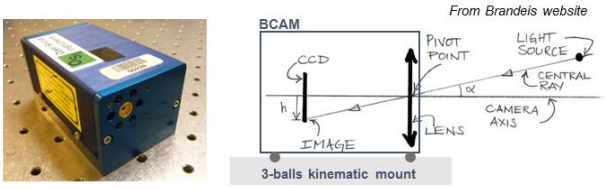


Figure 4 : BCAM camera (left), virtual camera (right)

Based on HIE-ISOLDE monitoring solution [11], the crab cavities alignment monitoring will rely on measurements of the bearings of several reflective targets placed on the helium tanks, using a set of BCAM placed on each side of the cryomodule, as shown in Figure 5.

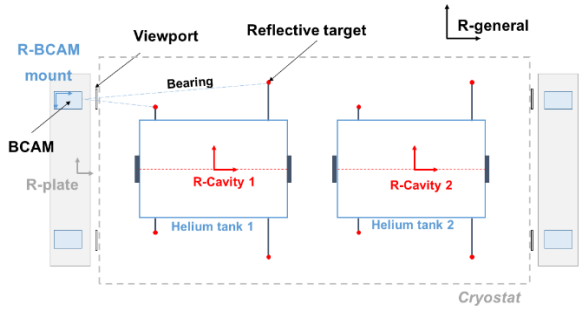


Figure 5 : BCAM alignment system: schematic (top view)

The bearing measurements will be expressed in several coordinate systems including a mount system: $R_{BCAM-MOUNT}$, a system linked to the plate: $R_{PLATE}$ and a general system: $R_{GENERAL}$.

The main purpose will be to measure the bearings of the whole reflective targets expressed in the general system, in order to define the main axis of both cavities, deduced from a fitting method.

# MEASUREMENTS PROCEDURE AND ANALYSIS

## *Position monitoring strategy*

The starting point relies on the entire fiducialisation of both cavities with a Coordinate Measurement Machine (CMM) in order to determine the mean axis of the cavities w.r.t. external references (i.e. fiducials).

Once the cavities will be running, the monitoring process will aim at calculating the minimum 6-parameters transformation (the current solution assumes 8 measurements which increases the redundancy) from the measurement performed with both monitoring systems, matched with initial CMM fiducialisation data. This approach will also require the detailed knowledge of the movements due to the thermal contraction in order to adjust the geometry of all system components by scale factors. An adequate calibration procedure shall be defined for both alignment systems.

To validate the strategy, a test setup based on the framework described above was built to study the feasibility and the accuracy of both approaches.

## *Test campaign*

The test setup concerns the absolute positioning of one helium tank represented by an aluminium structure carrying all the fiducials for FSI and BCAM measurements (cf. Figure 6).


Figure 6 : Test setup

The FSI measurement determines the distance between a ball mounted 1.5” reflector (centering to 0.0001 inch) to a FSI collimator, which is mounted on a kinematic mount providing a tip-tilt adjustment. The overall calculation includes 8 complementary FSI channels (4 per flange). A BCAM acquisition corresponds to images of reflective

targets made from S-LAH79 high index glass ball. A pair of two opposite BCAMs monitors the geometry of the structure from the acquisition of 8 ball lenses (4 per line of sight).

### *Coordinate systems*

The layout of the experiment is presented in Figure 7.

A general coordinate system: $R_{GENERAL}$ was defined in order to reference the FSI and BCAM acquisitions in a common frame for comparison of both alignment systems.

All the fiducials placed on the aluminium structure were measured using a CMM (micrometric uncertainty) and were expressed in the structure coordinate system: $R_{STRUCTURE}$ [8].

A coordinate system was connected to each collimator: $R_{FSI\ MOUNT}$ while each BCAM was installed on a 3-balls kinematic mount defining a BCAM coordinate system: $R_{BCAM-MOUNT\ A-B-C-D}$ [9].

Each kinematic BCAM mount was based on a metrological plate (plate A and B) measured by CMM measurements in the coordinate system:$R_{PLATE}$.

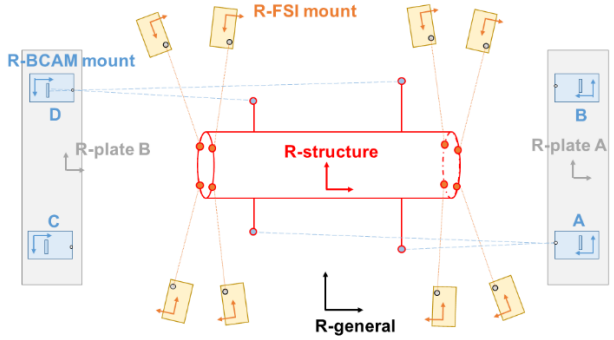


Figure 7 : Alignment framework

The main purpose of the test campaign was to assess the 6-parameters transformation to change from $R_{STRUCTURE}$ to $R_{GENERAL}$ deduced from both independent alignment systems.

## FSI ALIGNMENT STRATEGY

### *Calibration*

The FSI calibration consisted in determining the 3D-coordinates of the fibre end (i.e. focal point of the collimation lens, named hereafter as "zero point") as well as the direction of the laser beam expressed in $R_{FSI\ MOUNT}$ (cf. Figure 8).

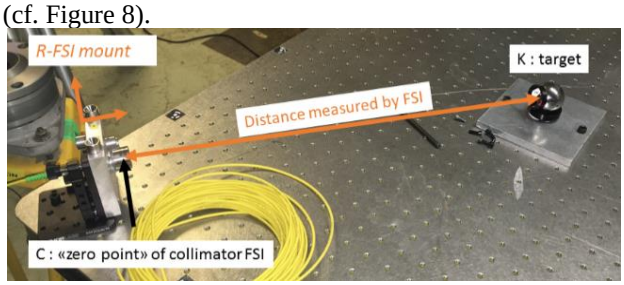


Figure 8 : Determination of the focal point ("zero point")

The distance measured with the FSI represents the distance between the focal point C and the reflectors Ki. A second frame shaped from the optical X-axis of the collimator was introduced (cf. Figure 9).

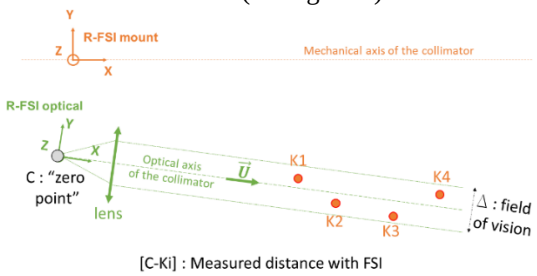


Figure 9 : Description of the frames of the collimator

The reflectors Ki were placed in the field of vision (Δ) of the collimator's lens in order to perform a distance acquisition. The Etalon™ software displayed the intensity of the reflected signal in percentage terms. A high percentage matches with a tight alignment, reached as soon as the target is close to the optical axis. The field of vision where the reflected signal intensity is upper than 15% (for Etalon software) represents a cylinder of 4 mm radius along the optical axis. A maximum percentage of intensity (± 1%) was kept within a cylinder of 0.200 mm of radius along the optical axis.

On this basis, the optical axis is described from a parametric equation of a straight line passing through the focal point, calculated from 4 observations (i):

$$\begin{pmatrix} X_{K_i} \\ Y_{K_i} \\ Z_{K_i} \end{pmatrix} = \begin{pmatrix} X_C \\ Y_C \\ Z_C \end{pmatrix} + \begin{pmatrix} U_X \\ U_Y \\ U_Z \end{pmatrix} * Dist_i \qquad (1)$$

Where $(X_{K_i}, Y_{K_i}, Z_{K_i})$ is the 3D-coordinates of the target expressed in the support frame (known from Laser Tracker measurements), $Dist_i$ is the distance to the target measured with the FSI, $(U_X, U_Y, U_Z)$ is the unit vector directed along the optical axis (unknown), and $(X_C, Y_C, Z_C)$ is the 3D-coordinates of the focal point (unknown).

$(U_X, U_Y, U_Z)$ and $(X_C, Y_C, Z_C)$ were estimated in the support frame, using the method of least squares.

Due to the configuration of the test setup, the precision achieved on the coordinate $X_C$ was much better than the precision on $Y_C$ and $Z_C$ coordinates: 10 µm ($X_C$) against about 1 mm ($Y_C$ and $Z_C$). The same tendency was observed for the determination of the vector U. The a-posteriori standard deviation on the distances was around 10 µm, which corresponds to the laser tracker accuracy used during the calibration. For the final project, a CMM will be used to calibrate the "zero-point" of the FSI collimator in order to achieve better accuracy.

### *Calculation*

Knowing the 3D-coordinates of the "zero point" of each FSI collimator (i), the distance (Di) measured with the FSI (i) can be expressed as follow:

$$D_i = \sqrt{\left(X_{C_i} - X_{T_i}\right)^2 + \left(Y_{C_i} - Y_{T_i}\right)^2 + \left(Z_{C_i} - Z_{T_i}\right)^2} \quad (2)$$

Where $(X_{C_i}, Y_{C_i}, Z_{C_i})$ are the 3D-coordinates of the "zero point" expressed in $R_{GENERAL}$ (known, deduced from calibration), and $(X_{K_i}, Y_{K_i}, Z_{K_i})$ are the 3D-coordinates of the reflective target (i) expressed in $R_{GENERAL}$.

$(X_{T_i}, Y_{T_i}, Z_{T_i})_{R_{GENERAL}}$ is unknown but can be deduced from:

$$\begin{pmatrix} X_{Ti} \\ Y_{Ti} \\ Z_{Ti} \end{pmatrix}_{R_{GENERAL}} = \begin{pmatrix} T_X \\ T_Y \\ T_Z \end{pmatrix} + [R] \begin{pmatrix} x_{Ti} \\ y_{Ti} \\ z_{Ti} \end{pmatrix}_{R_{STRUCTURE}} \quad (3)$$

Where $(x_{T_i}, y_{T_i}, z_{T_i})_{R_{STRUCTURE}}$ results from the CMM measurements carried out on the structure, $R = R_Z . R_Y . R_X$ and $T(T_X, T_Y, T_Z)$ are the parameters transformation to change from $R_{STRUCTURE}$ to $R_{GENERAL}$.

By combining the expressions (2) and (3), the parameters $(T_X, T_Y, T_Z, R_X, R_Y, R_Z)$ are assessed from 8 FSI observations and estimated using the least square method.

### *Results*

The adjusted parameters of the transformation converting $R_{STRUCTURE}$ to $R_{GENERAL}$ are presented in Table 1.

Table 1 : Parameters for FSI calculation

| Parameters | Value | Precision |
|---|---|---|
| $T_x$ (mm) radial | -2.585 | 0.021 |
| $T_y$ (mm) vertical | 269.799 | 0.009 |
| $T_z$ (mm) longitudinal | 154.424 | 0.028 |
| $R_x$ (rad) pitch | 0.006547 | 0.000030 |
| $R_y$ (rad) yaw | 0.011039 | 0.000072 |
| $R_z$ (rad) roll | 0.010422 | 0.000187 |

The a-posteriori standard deviation on the distances is of the order of 20 µm, which is twice the expected value.

This difference could come from the non-repeatable positioning of the fibre end w.r.t. to the focal point of the collimation lens, considering that the fibres were disconnected just after the calibration procedure and reconnected to the collimator for the test campaign. Although preliminary tests showed a good repeatability on the distance measurements, when the fibre is disconnected/reconnected to the collimator, additional tests should be carried out to confirm this result. Furthermore, the difference observed between the vertical and radial translation precisions (10 µm against 20 µm) is linked to the geometrical configuration of the FSI collimators placed around the structure.

To conclude, the 6-parameters precision meets the alignment constraints of the specifications.

## BCAM ALIGNMENT STRATEGY

### *In-situ calibration*

The 6-parameters transformation to change from the BCAM system $R_{BCAM-MOUNT}$ to $R_{GENERAL}$ was deduced from the Laser tracker measurements carried out on the metrological plates. The greatest uncertainties were observed on rotation parameters (a few hundred µrad), that might be caused by the determination of the mounting balls position.

In order to improve the rotation parameters, an in-situ calibration was performed making us of the light sources of a pair of opposite BCAMs (cf. Figure 10).

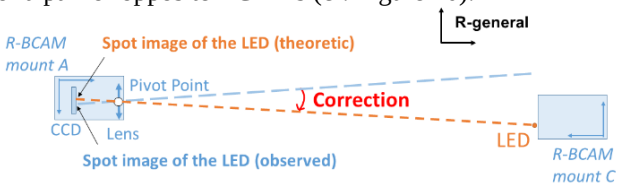


Figure 10 : BCAM in-situ calibration

The BCAM-A, opposite to BCAM-C, acquires the spot image of the LED of BCAM-C (and vice-versa).

Knowing the position of the LED of BCAM-C in $R_{BCAM-MOUNT-C}$ (given by manufacturer) and the transformation to $R_{GENERAL}$ (deduced by CMM measurement), the coordinates of the LED in $R_{GENERAL}$ can be estimate.

Knowing the reading of the BCAM-A in $R_{BCAM-MOUNT-A}$ and the transformation to $R_{GENERAL}$, one can calculate the coordinates of the pivot point and the spot image in $R_{GENERAL}$.

In a perfect case, the 3 points (Spot image observed, Pivot point and LED) should be aligned. Due to the uncertainty of the mounting ball positions, the rotation angles between $R_{BCAM-MOUNT}$ and $R_{GENERAL}$ are imprecise at few hundred µrad.

A correction was calculated from the comparison between the theoretical spot and the observed spot of the LEDs of the opposite BCAM.

### *Calculation*

Knowing the transformations to change from $R_{BCAM-MOUNT}$ to $R_{PLATE}$ and between $R_{PLATE}$ and $R_{GENERAL}$, the direction of the vectors $(\overrightarrow{BA})$ connecting the spot image and the pivot point of the whole reflective target can be expressed in the general system (cf. Figure 11). The zenith angle (φ) and the azimuth angle (θ) can be defined from the vectors' direction (spherical coordinate).

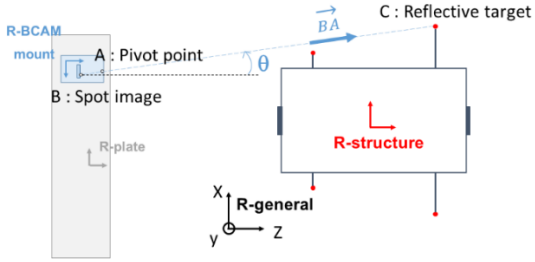


Figure 11 : BCAM calculation

The vector ($\overrightarrow{BC}$) linking the spot image to the reflective target must be collinear with the vector ($\overrightarrow{BA}$). $\overrightarrow{BA}$ and $\overrightarrow{BC}$ should have the same zenith (φ) and azimuth (θ) angles, expressed as follows:

$$\theta = tan^{-1}\frac{(X_{C_i}-X_{B_i})}{(Z_{C_i}-Z_{B_i})} \quad (4)$$

$$\varphi = \tan^{-1}\frac{(Y_{C_i}-Y_{B_i})}{\sqrt{(Z_{C_i}-Z_{B_i})^2+(X_{C_i}-X_{B_i})^2}} \quad (5)$$

The transformation from $R_{STRUCTURE}$ to $R_{GENERAL}$ is given by:

$$\begin{pmatrix} X_{Ci} \\ Y_{Ci} \\ Z_{Ci} \end{pmatrix}_{R_{GENERAL}} = \begin{pmatrix} T_X \\ T_Y \\ T_Z \end{pmatrix} + [R] \begin{pmatrix} x_{Ci} \\ y_{Ci} \\ z_{Ci} \end{pmatrix}_{R_{STRUCTURE}} \quad (6)$$

By combining the expressions (4), (5) and (6), the parameters ($T_X, T_Y, T_Z, R_X, R_Y, R_Z$) are calculated from 32 BCAM observations and estimated using the least square method.

### *Results*

The adjusted parameters of the transformation to change from $R_{STRUCTURE}$ to $R_{GENERAL}$ are presented in Table 2.

Table 2 : Parameters for BCAM calculation

| Parameters | Value | Precision |
|---|---|---|
| $\boldsymbol{T_x}$ (mm) radial | -2.624 | 0.026 |
| $\boldsymbol{T_y}$ (mm) vertical | 269.833 | 0.016 |
| $\boldsymbol{T_z}$ (mm) longitudinal | 155.839 | 0.622 |
| $\boldsymbol{R_x}$ (rad) pitch | 0.006536 | 0.000057 |
| $\boldsymbol{R_y}$ (rad) yaw | 0.011084 | 0.000057 |
| $\boldsymbol{R_z}$ (rad) roll | 0.010271 | 0.000083 |

The a-posteriori standard deviation on the azimuth angles is of the order of 45 µrad while the a-posteriori standard deviation on the zenith angles is of the order of 15 µrad. Although these values meet the precision given by the manufacturer (50 µrad), the significant difference between the a-posteriori standard deviations has to be investigated.

## AT401 ALIGNMENT STRATEGY

The laser tracker used for this test is the Absolute Tracker AT401 from Leica with an accuracy of ±15 µm + 6 µm/m (MPE) for the angular performance and ± 10 µm for the absolute distance.

### *Calculation*

The 6-parameters transformation to change from $R_{STRUCTURE}$ to the general system $R_{GENERAL}$ was assessed from the CMM measurements of the structure and the AT401 measurement.

### *Results*

The adjusted parameters of the transformation to change from $R_{STRUCTURE}$ to $R_{GENERAL}$ are presented in Table 3.

Table 3 : Parameters for AT401 calculation

| Parameters | Value | Precision |
|---|---|---|
| $\boldsymbol{T_x}$ (mm) radial | -2.596 | 0.002 |
| $\boldsymbol{T_y}$ (mm) vertical | 269.814 | 0.002 |
| $\boldsymbol{T_z}$ (mm) longitudinal | 154.459 | 0.004 |
| $\boldsymbol{R_x}$ (rad) pitch | 0.006535 | 0.000006 |
| $\boldsymbol{R_y}$ (rad) yaw | 0.011091 | 0.000006 |
| $\boldsymbol{R_z}$ (rad) roll | 0.010223 | 0.000014 |

## COMPARISON WITH THE AT401

The position of the structure axis in $R_{GENERAL}$ can be deduced from the transformation to change from $R_{STRUCTURE}$ to $R_{GENERAL}$ calculated from the three strategies (AT401, FSI, BCAM).

The comparison with the AT401 measurements is presented in Figure 12.

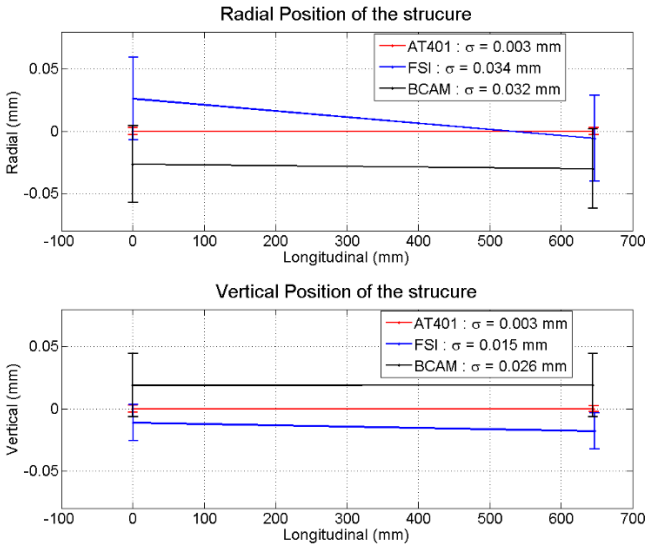


Figure 12 : Comparison with AT401

The radial and vertical positions of the extremity of the axis based on each strategy are very close, which confirms the precision and accuracy of all the strategies [12].

The AT401 strategy remains the most accurate (3 µm) but it cannot be used to align and monitor the cavities under vacuum and at cryogenic temperature, through a magnetic and thermal shielding.

The FSI strategy produces better accuracy in vertical (15 μm) than in radial (34 μm) because of the geometrical configuration of the FSI collimators around the structure. An accurate longitudinal position (30 μm) of the structure axis can be deduced from this calculation. The determination of the roll-rotation is accurate at 200 μrad.

The BCAM strategy gives an accurate radial and vertical position of the structure axis (30 μm). The roll-rotation was established at 80 μrad while the longitudinal position was imprecise at a few millimetres.

## CONCLUSION

Both alignment monitoring systems have been tested under standard conditions (room temperature, atmospheric pressure, no radiation) and their accuracy meets the alignment constraints of the specifications. Their results were compared to laser tracker measurement and the differences were insignificant.

The next stage will be the validation of the FSI system under vacuum and cryogenics. The FSI targets and the collimators were already tested with success regarding radiation aspect up to 10 MGy. Cryogenic tests are in progress.

## REFERENCES


[1] High-Luminosity Large Hadron Collider (HL-LHC). Preliminary Design Report, G. Apollinari, I. Béjar Alonso, O. Brüning, M. Lamont, L. Rossi, CERN-2015-005 (CERN, Geneva, 2015); http://cds.cern.ch/record/2116337

[2] I. Bejar et al., HiLumi LHC Technical Design Report, CERNACC-2015-0140 - Geneva: CERN, 2015; http://cds.cern.ch/record/2069130?ln=en

[3] L. Rossi, "LHC Upgrade Plans: Options and Strategy", Proceedings of IPAC2011, San Sebastián, Spain, 01/09/2011,pp.908-912, http://accelconf.web.cern.ch/AccelConf/IPAC2011/papers/tuya02.pdf

[4] R. Calaga, "Crab cavities for the LHC upgrade", proceedings of Chamonix 2012 workshop on LHC, 2012

[5] M.Sosin, Position Monitoring system for HL-LHC crab-cavities, International Particle Accelerator Conference, 2016

[6] M.S. Warden, Absolute distance metrology using frequency swept lasers, these proceedings, 2011

[7] http://www.etalon-ag.com/

[8] http://alignment.hep.brandeis.edu/Devices/BCAM/

[9] G.Kautzmann, J-C Gayde, Y.Kadi, Y.Leclercq, S.Waniorek, L.Wiliams, "The HIE-ISOLDE Alignment and monitoring system", International Workshop on Accelerator Alignment, 2012

[10] V.Rude, T.Dijoud, "Fiducialisation of the prototype", EDMS: 1718086, 2016

[11] V.Rude, T.Dijoud, "Fiducialisation and calibration of FSI collimators", EDMS: 1718389, 2016

[12] V.Rude, "Simulation: Position of FSI collimator", EDMS: 1719029, 2016